

Some Observations of Thunderstorm-Induced Low-Level Wind Variations

R. Craig Goff*

National Severe Storms Laboratory, Norman, Okla.

Strong low-level horizontal winds, wind shear, and severe turbulence are frequently associated with the cold air outflow of mature, intense thunderstorms. The outflow is a product of in-cloud processes that bring massive quantities of air down to ground level, then horizontally ahead of the storm. The relatively shallow, fast-moving thunderstorm outflow airmass resembles a density current. The airmass leading edge (called the gust front) is a sharp, highly baroclinic windshift zone. Imbedded within the outflow airmass are secondary surges of outflow from the thunderstorm; each is characterized by strong horizontal shears. In addition to strong horizontal winds and shears, the gust front and subsequent outflow surges are typically characterized by large updrafts and downdrafts. All these wind factors make low-level aircraft operation difficult and often unsafe. Buildings and other stationary structures vulnerable to high winds may also be adversely affected. The character of a thunderstorm outflow case is described using data from a multilevel 461-m meteorological tower in central Oklahoma. Statistical information is presented which verifies that an aircraft on takeoff or approach can be frequently affected by headwind loss coupled with downdrafts (short landing on approaches) and these conditions are more prevalent at lower tower levels.

I. Introduction

THE severe thunderstorm with attendant high winds, strong turbulence, and damaging hail is an atmospheric phenomenon to be avoided by airborne vehicles. The precipitating portion of the storm is detectable by conventional radar or visual observations but there is evidence^{1,5} that thunderstorm-induced strong winds, high shear, and turbulence zones associated with the storm's cold air outflow exist up to 30 km ahead of the advancing storm. The outflow is often precipitation-free, precluding detection by operational radars. Visual observations of the outflow's leading edge may be obscured by clouds or darkness.

The thunderstorm outflow is a low-level, shallow layer of high momentum air more dense than its environment. Its source is at mid-tropospheric levels. Here, dry air is entrained into the storm's falling precipitation, is cooled by evaporation, becomes negatively buoyant and descends to the ground. At the surface, the leading edge of the outflow (gust front) propagates out ahead of the storm, moving several kilometers away from the rainfall onset as the storm reaches maturity.

In recent studies,^{3,5} the character of the outflow's leading edge has been described using data from a 461-m meteorological tower in Oklahoma. In the 1975 study, gust front data from twenty cases were analyzed. One of these cases is selected and the analysis expanded to include the complete internal structure of the outflow.

II. Data Sources and Objective Analysis

The meteorological tower is a data facility of the National Severe Storms Laboratory (NSSL) in Norman, Okla. The tower is the KTVY (formerly WKY-TV) television transmitter located about 38 km north of NSSL in a sparsely populated area north-northeast of Oklahoma City. In 1971 the tower was equipped with horizontal wind and temperature sensors at seven levels (26, 45, 89, 177, 266, 355, and 444 m) and with vertical velocity sensors at three levels (26, 177, and 444 m). Data were collected at 10 sec intervals and stored on magnetic

tape. Descriptions of the sensors are contained in reports by Carter² and Goff and Zittel.⁴

Multilevel time series data are objectively analyzed by determining grid values at 50 m vertical intervals from 0 to 450 m using linear interpolation and extrapolation. The resulting arrays for the three components of the wind and the potential temperature are machine contoured. These contoured time-height cross sections for June 7, 1971, are shown in the bottom four panels of Fig. 1. The data are unfiltered. The horizontal wind component normal to the front and vertical velocity are combined to produce the streamline analysis in the top panel. There is considerably less detail in the temperature section compared to the wind sections because the temperature sensors have longer time constants than response times of either wind sensor.

Each section starts at 1935 CST and ends at 2013 CST. Time increases from right to left. Units are mks and K. A 1 km scale length using a Galilean transformation ($\Delta x = -c\Delta t$) appears in the upper right of the diagram. The scale length is useful near the gust front but becomes less reliable more than a few kilometers either side of the front since the velocity of tower layer features are not known with any certainty except in the frontal zone.

Figure 2 is a radar PPI diagram for 1945 CST on June 7, 1971, the time of the gust front passage at the tower. The NSSL radar is a conventional 10 cm model WSR-57 with rainfall intensity contouring. Most of the return within the first range mark is ground clutter. Range marks are at 20 N. mi. intervals. Isolated ground return on the 20 N. mi. range mark at 358° azimuth is a cluster of four transmitter towers, one of which is the KTVY tower. Northwest of the tower is the large thunderstorm cell (cell A) producing the cold air outflow. Horizontal wind components in Fig. 1 are plotted relative to the coordinate system shown in Fig. 2. The origin is fixed to the ground, u - and v -components are normal and parallel to the frontal axis, respectively.

III. Data Interpretation

The onset of cold air outflow from cell A at 1945 CST is represented in Fig. 1 by a sharp shear zone in the u -component (wind speed normal to the front and relative to the ground), a temperature discontinuity that lags behind the windshift and a 1 km wide updraft in advance of the front followed by large downdrafts near the surface behind the front. Most of the horizontal wind variation occurs in the component of the

Received June 30, 1976; presented as Paper 76-388 at the AIAA 9th Fluid and Plasma Dynamics Conference, San Diego, Calif., July 14-16, 1976; revision received Dec. 13, 1976.

Index categories: Aircraft Gust Loading and Wind Shear; Atmospheric, Space, and Oceanographic Sciences.

*Research Meteorologist, National Aviation Facilities Experimental Center, FAA, Atlantic City, N.J.

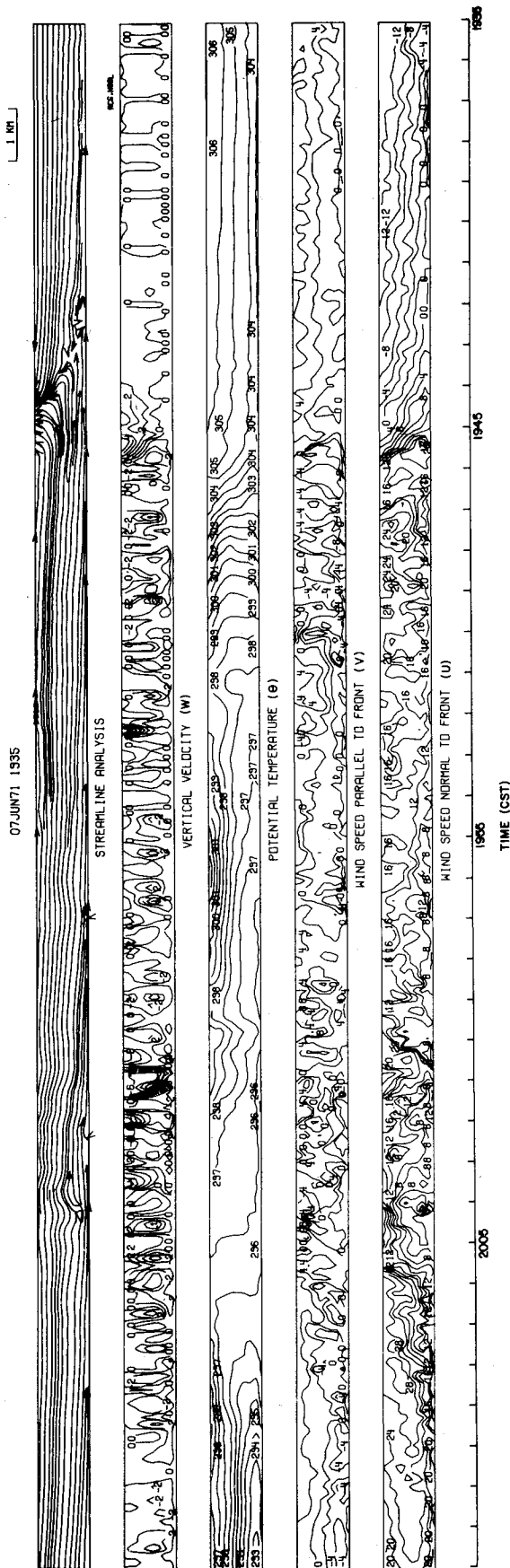


Fig. 1 Time-height cross section of wind and temperature in the tower layer. Units are mks and K. Streamlines are drawn using windspeed normal to front (relative to ground, u) and vertical velocity (w). A 1 km time-to-space representative length is shown in the upper right. Gust front occurs at 1945. Outflow is moving from left to right. Thunderstorm is on extreme left and is moving toward right. Coordinate system is shown in Fig. 2.

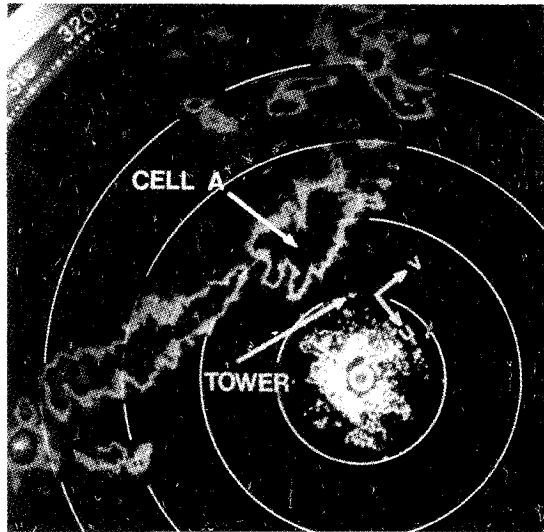


Fig. 2 NSSL's 10 cm surveillance radar diagram for 1945 CST, June 7, 1971. Tower position and storm (cell A) producing outflow are indicated. Echo contouring corresponds to powers (x) of $10^x \text{ mm}^6/\text{m}^3$ reflectivity (roughly proportional to precipitation intensity). Range marks (circles) are at 20 N. mi. intervals.

wind normal to the front. Although the horizontal wind field parallel to the front (v -component) is not smooth, total variation throughout the whole section is only about 16 m/sec compared to a 40 m/sec variation in the wind field normal to the front (u -component). Therefore, we will not discuss the v -component field or its derivatives.

The squall line containing cell A is moving about 10 m/sec toward 140° azimuth. Though the leading edge of the outflow is a curved surface in front of cell A, the portion passing the tower site at 1945 CST is also propagating toward 140° at 11.8 m/sec.

Two other surges of high-momentum air appear in the outflow airmass from cell A at 2000 and 2004 CST (Fig. 2). Rainfall begins at 2009, a few kilometers behind the surge at 2004. Granted no cause and effect relationship is definite from the tower data alone, obviously some high-level in-storm physical processes are the source for these surges. Both surges are characterized by a strong shear zone in the u -component and large variations in the vertical velocity. A downdraft in excess of 11 m/sec is observed at the 177 m level at 2001 CST.

The potential temperature time-height section reveals important information about the variation in depth of the cold air outflow. Without evaporation or condensation, an air parcel moving over the outflow will retain a constant potential temperature (or entropy); i.e., its potential temperature (θ) is conserved ($d\theta/dt=0$). With this assumption, the local derivative is simply a function of advected undulations in the quasihorizontal top of the cold air outflow. Such undulations are schematically illustrated by the wavy heavy line (Fig. 3) representing the top of the outflow. Figure 3 is a cross section of the outflow drawn to the same scale as the observations in Fig. 1. All detail in Fig. 3 above 450 m is inferred, whereas detail below 450 m is drawn to match the observations in Fig. 1. The lower portion of the transition layer from cold to warm air near the top of the outflow is characterized by a positive thermal gradient to above 300 m (Fig. 1). The wind transition from cold air flowing away from the storm to warm air flowing toward the storm is at the top of the inversion and is not observed in Fig. 1; but the potential temperature field at 1955, 2000, and 2009 CST indicates the vertical wind shear zone in the gust front envelope is only a few hundred meters above the tower top. The heavy lines in Fig. 3 also denote the sloping horizontal wind shear zones of the front at 1945 and subsequent outflow surges at 2000 and 2004 CST. In the cross section (Fig. 3), arrows represent

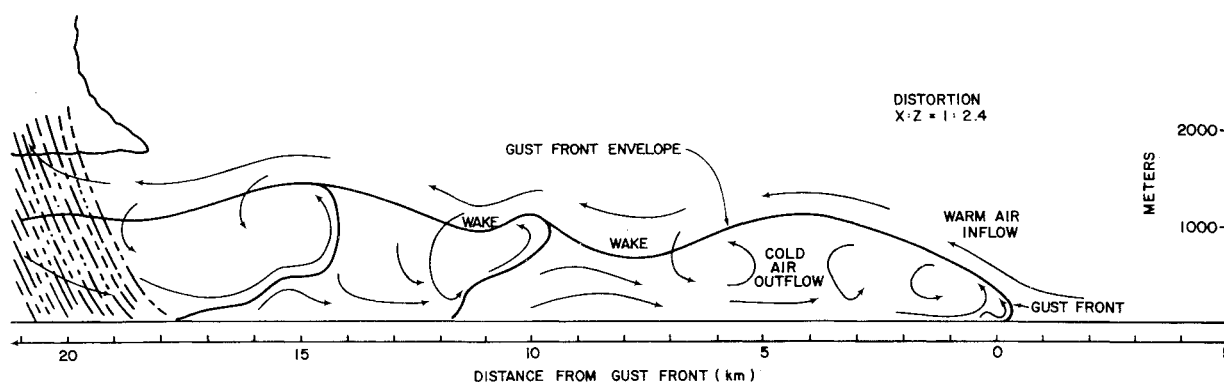


Fig. 3 Schematic diagram of complete outflow structure based on data in Fig. 1 (see text). Distances from gust front are based on time-to-space conversion $\Delta x = -c\Delta t$. Streamlines are drawn relative to gust front and secondary surge boundaries. Streamlines do not match those plotted relative to ground in Fig. 1.

streamlines. However, relative to the horizontal wind shear boundaries the flow is not steady-state so streamlines do not coincide with fluid trajectories.

Figure 3 indicates the prestorm warm moist air is displaced upward by the more dense outflow from the thunderstorm. The mechanical forcing occurs in a 1 km wide band in advance of the gust front. After rising about 800 m over the head, gravitational instability forces the uplifted air down in the wake of the gravity current (7 km from gust front) and horizontal divergence assists entrainment of warm air across the inversion boundary into the cold outflow. This wake, then, is a highly turbulent zone frequently characterized by large shears in the horizontal wind and large oscillations in vertical motion. Similar characteristics are observed in the secondary outflow surges. Horizontal divergence is so strong in the wake of the second surge (11 km from gust front) that a large volume of air descends almost to the surface.

IV. Wind Variations in the Outflow Perturbed Boundary Layer

It is clear that aircraft preparing to land or take off will encounter strong shear at low levels in cold air outflows resembling the June 7 1971 case. We have been discussing the observations of this case in a qualitative way and now present statistical information to verify boundary-layer wind variations.

For the purposes of the following discussion it will be assumed a hypothetical runway is oriented 320° to 140° (true). Therefore, an aircraft will penetrate the outflow in one of three flight configurations: 1) Takeoff toward northwest (left in Fig. 3) penetrating deeper into the cold air, rising above the outflow through the gust front envelope. The intended flight path assumes the gust front has passed the airport and the surface wind is generally from the northwest but also assumes the pilot will not fly into the precipitating storm. 2) Landing toward the northwest penetrating the gust front from the warm air side to the cold air side. The flight path assumes the gust front has passed the airport. 3) Landing toward the southeast (right in Fig. 3), penetrating the cold air outflow top some distance from the touchdown point, descending while in the outflow, passing through the gust front from the cold air side to the warm air side, and landing in the warm air. The path assumes the gust front has not reached the airport at the approach decision time.

Aircraft that take off toward the southeast before the gust front passage do not encounter the cold air outflow since they are moving away from the gust front.

Although aircraft may encounter strong shear anywhere in proximity to the cold air outflow, such encounters are more dangerous closer to the surface. Close to the ground, turbulence, strong downdrafts, and changes in headwind can adversely affect an aircraft to a point where recovery might be impossible. Such conditions were possible in the June 7 1971 case.

Figures 4a-c are wind matrices for 26, 177, and 444 m tower levels for all three flight configurations. The 227 point data sample for the matrices is obtained from the same time series used in the time-height analysis (Fig. 1). Matrices are bivariate frequency distributions of vertical velocity versus horizontal wind shear. Horizontal wind shear class intervals represent the change in horizontal wind speed (u -component in Fig. 1) an aircraft would experience in 100 m of flight, that is

$$\Delta u_a / \Delta x = (1/c) (\Delta u_g / \Delta t) \quad (1)$$

where c is the speed of the gust front, $\Delta t = 10$ sec, $\Delta x = 100$ m, and u_a and u_g represents winds in coordinate systems oriented to the aircraft (a) and the ground (g).[†]

In this analysis the effect of vertical shear has been ignored since the small slope of the aircraft glide path (typically 3° from the horizontal) implies the vertical shear ($\Delta u / \Delta z$) will generally influence the aircraft less than horizontal wind shear ($\Delta u / \Delta x$). It is also assumed that the outflow is two-dimensional; i.e., $\partial / \partial y = 0$. This assumption is justifiably suspect. Notwithstanding this point, the statistical results to be shown are believed representative of other slices through this outflow.

Figures 4 a-c show that downdrafts coupled with a loss of headwind or increase in tailwind occur more frequently at all three tower levels than any other combination of vertical velocity and change in headwind/tailwind. Each matrix is divided into four quadrants, and the four central class intervals (within the diamonds) are ignored. Table 1 reveals that of the remaining observations, 69 (36.7%) are in the headwind loss/tailwind gain/downdraft quadrant (IV) at 26 m compared to 58 (28.9%) and 52 (30.2%) observations at 177 and 144 m, respectively. Clearly, the condition experienced in quadrant IV favoring an aircraft loss in altitude is generally the most prevalent. The condition occurs more frequently at the lowest tower level than at higher levels. Table 1 shows that updrafts coupled with headwind gain/tailwind loss (quadrant II), conditions that might cause an aircraft to rise above the intended glide path, are observed comparatively infrequently: 15.4, 17.4, and 26.1% at 26, 177, and 444 m, respectively.

Exact aircraft response is not known for quadrants I and III, because possible loss of lift through horizontal shear is compensated by updrafts (quadrant I). The converse holds for quadrant III.

V. Conclusions, Recommendations, and Future Study

The cold air outflow preceding a thunderstorm contains shear and turbulence zones which may adversely affect an aircraft. The strength of wind shear does not appear to be a

[†]The formula used in the original manuscript⁶ is incorrect as were results based on its application.

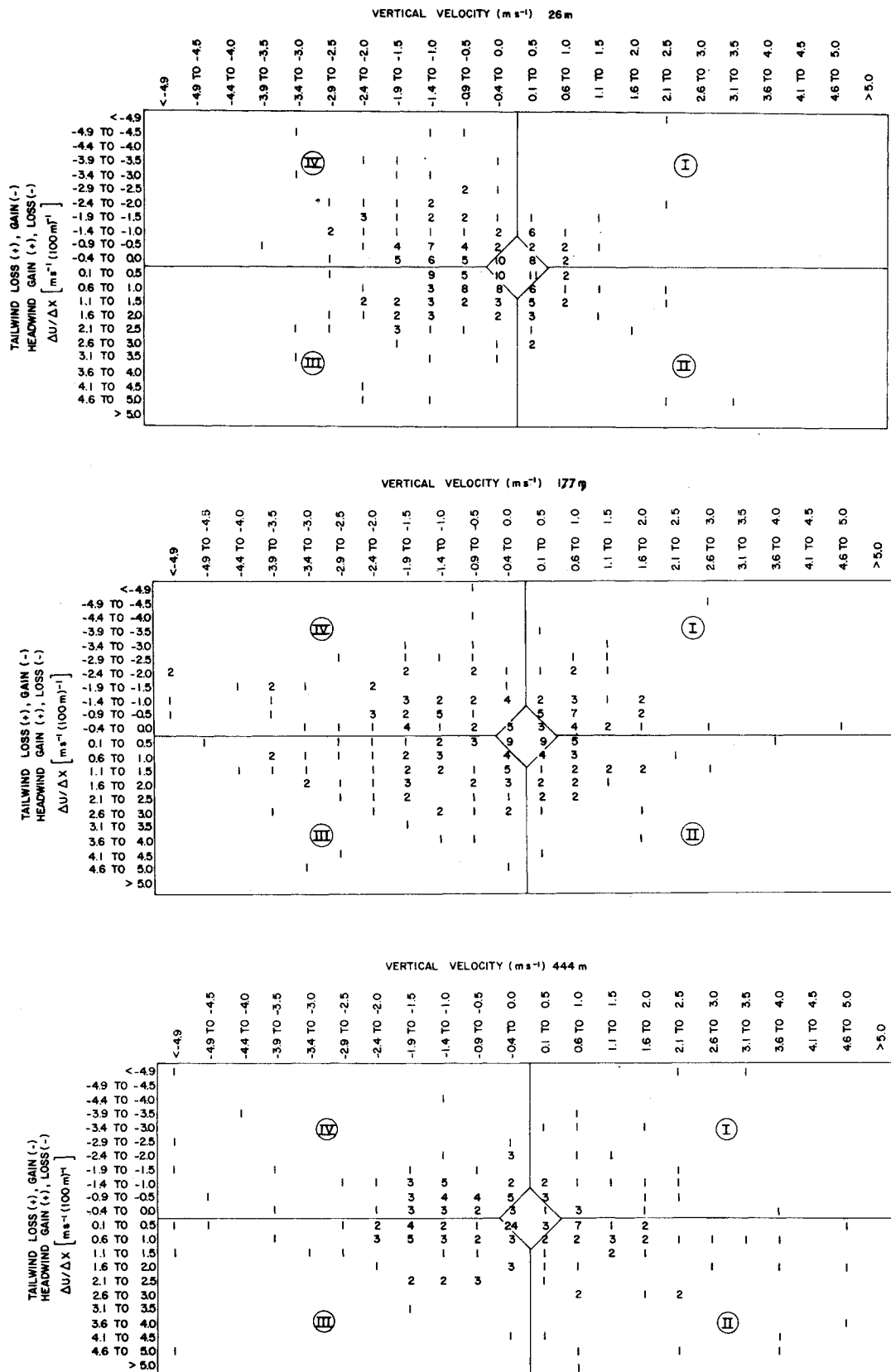


Fig. 4 Bivariate frequency distribution of vertical velocity and headwind/tailwind change for three tower levels: a) 26 m, b) 177 m, and c) 444 m. Sample size (227 data points) includes all data contoured in u and w panels in Fig. 1.

Table 1 Percent of observations in critical quadrants for any flight configuration (excluding central class intervals)

Meters	Tailwind gain/headwind loss and downdraft (quadrant IV) = > decreased lift	Tailwind loss/headwind gain and updraft (quadrant II) = > increased lift
26	36.7	15.4
177	28.9	17.4
444	30.2	26.1

function of the storm's intensity (Goff, unpublished data). Storm horizontal wind shears frequently accompany wind discontinuities associated with surges of high-momentum air from the thunderstorm. There can be any number of surges internal to one outflow.

It may be necessary to stipulate a wider danger zone around the thunderstorm for aircraft operations, at least until operational sensors are available to detect low-level turbulence and wind shear in the flight path. For example, with the meteorological information presently available to pilots and ground control personnel, an assessment of atmospheric conditions in the case presented might result in clearance given to aircraft to land or take off before adverse weather (precipitation associated) actually was observed at the airport. Even with reliable operational sensors, it may become necessary to discourage aircraft operations in a wider zone around the thunderstorm than guidelines presently recommended.

A three-dimensional analysis of the whole subcloud layer has yet to be undertaken. However, NSSL is embarking on such a study in its 1976 and 1977 spring data collection programs. Tower data will be combined with microwave Doppler and aircraft data to better define three-dimensional characteristics of the subcloud region in advance of the convective storm.

Acknowledgment

This research was supported by the Federal Aviation Administration Contract Number DOT-FA76-AWI-622. The author appreciates the assistance of C. Clark, J. Farris, L. Johnson, and advice from Dr. R. Alberty and J.T. Lee, all of the National Severe Storms Laboratory.

References

- ¹Byers, H.R. and Braham, R.R. Jr., *The Thunderstorm*, U.S. Government Printing Office, Washington, D.C., 1949, p.287.
- ²Carter, J.K., "The Meteorologically Instrumented WKY-TV Tower Facility," NOAA Tech. Memo ERL-NSSL, No. 50, 1970.
- ³Charba, J., "Application of Gravity-Current Model to Analysis of Squall Line Gust Front," *Monthly Weather Review*, Vol. 101, Feb. 1974, pp. 140-156.
- ⁴Goff, R.C. and Zittel, W.D., "The NSSL/WKY-TV Tower Data Collection Program: April-July 1972," NOAA Tech. Memo ERL-NSSL, No. 68, 1974.
- ⁵Goff, R.C., "Thunderstorm-Outflow Kinematics and Dynamics," NOAA Tech. Memo. ERL-NSSL, No. 75, 1975.
- ⁶Goff, R.C., "Some Observations of Thunderstorm-Induced Low-Level Wind Variations," AIAA Paper 76-388, San Diego, July 1976.

From the AIAA Progress in Astronautics and Aeronautics Series

SPACECRAFT CHARGING BY MAGNETOSPHERIC PLASMAS—v. 47

Edited by Alan Rosen, TRW, Inc.

Spacecraft charging by magnetospheric plasma is a recently identified space hazard that can virtually destroy a spacecraft in Earth orbit or a space probe in extra terrestrial flight by leading to sudden high-current electrical discharges during flight. The most prominent physical consequences of such pulse discharges are electromagnetic induction currents in various on-board circuit elements and resulting malfunctions of some of them; other consequences include actual material degradation of components, reducing their effectiveness or making them inoperative.

The problem of eliminating this type of hazard has prompted the development of a specialized field of research into the possible interactions between a spacecraft and the charged planetary and interplanetary mediums through which its path takes it. Involved are the physics of the ionized space medium, the processes that lead to potential build-up on the spacecraft, the various mechanisms of charge leakage that work to reduce the build-up, and some complex electronic mechanisms in conductors and insulators, and particularly at surfaces exposed to vacuum and to radiation.

As a result, the research that started several years ago with the immediate engineering goal of eliminating arcing caused by flight through the charged plasma around Earth has led to a much deeper study of the physics of the planetary plasma, the nature of electromagnetic interaction, and the electronic processes in currents flowing through various solid media. The results of this research have a bearing, therefore, on diverse fields of physics and astrophysics, as well as on the engineering design of spacecraft.

304 pp., 6 x 9, illus. \$16.00 Mem. \$28.00 List

TO ORDER WRITE: Publications Dept., AIAA, 1290 Avenue of the Americas, New York, N. Y. 10019